JOURNAL OF SOLID STATE CHEMISTRY 110, 256–263 (1994)

The Phosphoniobate $RbNb_2PO_8$: An Ordered Substitution of PO_4 Tetrahedra for NbO_6 Octahedra in the HTB Structure

A. Leclaire, M. M. Borel, A. Grandin, and B. Raveau

Laboratoire CRISMAT, Associé au CNRS, ISMRA, Université de Caen, Boulevard du Maréchal Juin, 14050 Caen Cedex, France

Received May 3, 1993; in revised form September 13, 1993; accepted September 15, 1993

A new phosphoniobate, $RbNb_2PO_8$, with an intersecting tunnel structure, has been synthesized. It crystallizes in the *Pnma* space group with $a = 13.815(1)$ Å, $b = 15.884(2)$ Å, $c = 12.675(2)$ Å, and $Z = 16$. The full matrix least-squares refinement led to $R = 0.041$ and $R_w = 0.050$. The host lattice is derived directly from that of the hexagonal tungsten bronzes (HTB) by an ordered substitution of PO_4 tetrahedra, forming two sorts of tunnels running along b and a, respectively, where the Rb^+ ions are located. The first type of tunnel results from the stacking of six-sided HTB-type rings ($5NbO_6$ octahedra + $1PO_4$ tetrahedron) with seven-sided rings ($4NbO_6$ octahedra + $3PO_4$ tetrahedra), whereas the second type of tunnel consists of brownmillerite rings ($4NbO_6$ octahedra + 2 PO_4 tetrahedra). © 1994 Academic Press, Inc.

INTRODUCTION

The investigations of the phosphates of transition elements performed these last 12 years have shown the great ability of the PO_4 tetrahedra to accommodate octahedral host lattices. The first series was discovered with the phosphate tungsten bronzes (1, 2), the frameworks of which derive from the perovskite structure by association of ReO_3-type layers with PO_4 or P_2O_7 groups. The second series was more recently observed for mixed valent niobium phosphates, the host lattice of which is closely related either to the tetragonal tungsten bronze (TTB) structure as for $KNb_3P_3O_{15}$ (3) and $Na_6Nb_8P_5O_{35}$ (4), or to the hexagonal tungsten bronze (HTB) structure, as shown for the bronzes $(K_3Nb_6P_4O_{26})_n \cdot KNb_2PO_8$ (5–7) and the oxide $Ca_{0.5}Cs_2Nb_6P_3O_{24}$ (8). The latter studies suggest that the Rb–Nb–P–O system is a good candidate for the generation of new original tunnel structures related to the HTBs owing to the size of rubidium, which is intermediate between those of potassium and cesium. The present paper deals with the synthesis and crystal structure of a new monophosphate of pentavalent niobium, $RbNb_2PO_8$, derived from the HTB structure by an ordered substitution of PO_4 tetrahedra for NbO_6 octahedra.

SYNTHESIS

Single phase powder samples and single crystals of $RbNb_2PO_8$ were prepared from $RbNO_3$, $H(NH_4)_2PO_4$, and Nb_2O_5 in appropriate proportions. The mixtures were mixed and heated in a platinum crucible to 653 K in air to decompose the $H(NH_4)_2PO_4$ and $RbNO_3$.

In order to obtain the pure phase, the samples were then ground and heated for 1 day to 1273 K in air in a platinum crucible and quenched at room temperature. The resulting product was a white microcrystalline powder. Single crystals of $RbNb_2PO_8$ were grown from the mixture obtained at 653 K, sealed in an evacuated silica ampoule, heated to 1273 K for 2 months, and quenched at room temperature. Some colorless crystals were extracted from the mixture. The microprobe analysis of these crystals confirmed the composition $RbNb_2PO_8$, in agreement with the structure determination.

The powder X-ray diffractogram registered with a PW 3710 Philips diffractometer was indexed in an orthorhombic cell (Table 1) with the parameters obtained from the single crystal study.

STRUCTURE DETERMINATION

A colorless transparent crystal of $RbNb_2PO_8$ with dimensions 0.077 × 0.064 × 0.064 mm was selected for the structure determination. The cell parameters, reported in Table 2, were determined and refined by diffractometric techniques at 294 K with a least-squares refinement based on 25 reflections with $18 < \theta < 22°$. The systematic absences $k + l = 2n + 1$ for $0\,k\,l$ and $h = 2n + 1$ for $h\,k\,0$ are consistent with the space groups *Pnma* (No. 62) and $Pn2_1a$ (other setting of $Pna2_1$ No. 33).

The Harker peaks present in the Patterson function are characteristic of the centrosymmetric space group *Pnma*. The data were collected on a CAD4 Enraf–Nonius automatic diffractometer with the measurement parameters reported in Table 2. The reflections were corrected for Lorentz and polarization effects. No absorption correc-

0022-4596/94 $6.00

TABLE 1
Interreticular Distances for $RbNb_2PO_8$

h k l	d_{calc}	d_{obs}	I	h k l	d_{calc}	d_{obs}	I
0 1 1	9.90	9.92	13	1 5 1	3.007	3.008	6
1 1 1	8.05	8.05	8.5	4 1 2	2.979	2.981	14
2 1 0	6.34	6.35	13	2 3 3	2.979		
0 0 2	6.34			2 5 0	2.886	2.884	14
2 0 1	6.066	6.066	10	4 3 1	2.820	2.818	6
2 0 2	4.670	4.662	12	2 5 1	2.814		
1 2 2	4.662			2 4 3	2.668	2.670	34
1 3 1	4.605	4.604	5	4 3 2	2.631	2.628	10
2 3 0	4.202	4.207	4.5	2 5 2	2.626		
3 1 1	4.177	4.179	7.5	3 0 4	2.610	2.608	20
0 1 3	4.081	4.082	22	4 4 0	2.606		
0 4 0	3.970	3.970	74	3 2 4	2.479	2.479	13
2 0 3	3.604	3.605	6	0 4 4	2.475		
2 1 3	3.514	3.511	6	5 2 2	2.413	2.412	12
4 0 0	3.455	3.447	18	4 4 2	2.410		
2 4 0	3.442			0 6 4	2.030	2.029	10
0 4 2	3.364	3.366	59	5 2 4	2.014	2.014	11
2 4 1	3.322	3.321	66	0 8 0	1.985	1.986	59
1 4 2	3.269	3.266	23	2 7 3	1.920	1.921	10
4 1 1	3.262			3 0 6	1.920		
4 2 0	3.168	3.170	50.5	6 4 2	1.900	1.900	10
0 0 4	3.167			3 2 6	1.866	1.866	10
3 0 3	3.113	3.114	27.5	6 5 0	1.865		
1 0 4	3.087	3.099	12.5	2 8 2	1.827	1.825	12
3 1 3	3.055	3.055	12	3 8 1	1.804	1.803	27
4 0 2	3.033	3.033	100	6 4 3	1.802		

TABLE 2
Summary of Crystal Data, Intensity Measurements, and Structure Refinement Parameters for $RbNb_2PO_8$

Crystal data	
Space group	*Pnma*
Cell dimensions	a = 13.815 (1) Å
	b = 15.884 (2) Å
	c = 12.675 (2) Å
Volume	2781.3(9) $Å^3$
Z	16
d_{calc}	4.11
Intensity measurements	
$\lambda(MoK\alpha)$	0.71073 Å
Scan mode	ω–2/3 θ
Scan width (°)	1.04 + 0.35 tan θ
Slit aperture (mm)	1.05 + tan θ
Max θ (°)	42°
Standard reflections	3 (every 3000 sec)
Reflections measured	10,536
Reflections with $I > 3\sigma$	1,830
$\mu(mm^{-1})$	10.2
Structure solution and refinement	
Parameters refined	130
Agreement factors	R = 0.041, R_w = 0.050
Weighting scheme	$w = f(\sin \theta/\lambda)$
Δ/σ max	<0.02
$\Delta\rho$ ($e/Å^{-3}$)	2.8

tions were performed. The small dimensions of the crystal allowed us to obtain only 1830 reflections with $I > 3\sigma(I)$ out of the 10,536 reflections measured, so that only the thermal factors of the fully occupied Nb and Rb sites were refined anisotropically, the others remaining isotropic.

The structure was discovered using the heavy atom method. Two of the independent niobium sites, Nb(1) and Nb(2), were found to be split into two close sites (labeled *a* and *b*) with an occupancy factor of $\frac{1}{2}$ and located above and below the basal plane of their ideal octahedra. The refinement of the atomic parameters led to R = 0.041 and R_w = 0.050 for the atomic parameters listed in Table 3.

DESCRIPTION OF THE STRUCTURE AND DISCUSSION

The projection of the structure of this phosphoniobate along **b** (Fig. 1) shows that the host lattice $[Nb_2PO_8]_\infty$ consists of corner-sharing NbO_6 octahedra and PO_4 tetrahedra forming large tunnels running along **b**. In this framework, each PO_4 tetrahedron shares its four apices with four different NbO_6 octahedra, whereas each NbO_6 octahedron is linked to four NbO_6 octahedra and two PO_4 tetrahedra.

In fact, the $[Nb_2PO_8]_\infty$ framework is directly derived from the hexagonal tungsten bronze (HTB) of Magneli (9)

TABLE 3
Positional Parameters and Their Estimated Standard Deviations

Atom	x	y	z	B(Å^2)
Nb(1a)	0.0186(2)	0.3893(1)	0.0208(2)	0.31(3)
Nb(1b)	0.0186(2)	0.3593(1)	0.0223(2)	0.39(3)
Nb(2a)	−0.0086(1)	0.3581(1)	0.4966(2)	0.32(3)
Nb(2b)	−0.0057(2)	0.3872(1)	0.5018(2)	0.37(3)
Nb(3)	0.10732(8)	0.63122(8)	0.22994(8)	0.33(1)[a]
Nb(4)	0.26008(7)	0.36910(8)	0.47253(8)	0.33(1)[a]
Rb(1)	0.3599(2)	0.75	0.2430(3)	2.39(5)[a]
Rb(2)	0.2572(2)	0.25	0.1552(2)	2.30(4)[a]
Rb(3)	0.3547(1)	0.5001(1)	0.2190(2)	2.04(3)[a]
P(1)	0.0998(2)	0.4081(2)	0.2696(3)	0.47(4)
P(2)	0.2425(2)	0.5905(2)	0.4460(2)	0.30(4)
O(1)	0.	0.5	0.	1.3(2)
O(2)	−0.1080(7)	0.3756(7)	0.0794(7)	0.7(1)
O(3)	0.022(1)	0.25	0.015(1)	0.9(2)
O(4)	0.0790(7)	0.3626(7)	0.1635(7)	0.8(1)
O(5)	0.1636(6)	0.3708(8)	−0.0168(8)	1.0(1)
O(6)	−0.0073(6)	0.3694(8)	−0.1328(7)	0.6(1)
O(7)	0.1248(7)	0.3623(7)	0.5190(8)	0.9(1)
O(8)	0.0122(7)	0.3879(6)	0.3420(7)	0.7(1)
O(9)	−0.0272(7)	0.3620(7)	0.6507(7)	0.8(1)
O(10)	0.	0.5	0.5	1.4(2)
O(11)	−0.1591(7)	0.3826(6)	0.4805(8)	0.8(1)
O(12)	−0.027(1)	0.25	0.473(1)	1.3(2)
O(13)	0.1301(9)	0.75	0.224(1)	0.5(2)
O(14)	0.105(1)	0.5024(8)	0.2475(9)	1.7(2)
O(15)	0.2265(6)	0.6210(6)	0.3330(7)	0.6(1)
O(16)	0.2056(7)	0.6167(6)	0.1133(7)	0.7(1)
O(17)	0.2504(9)	0.4949(7)	0.4480(8)	1.3(2)
O(18)	0.1941(7)	0.3731(8)	0.3160(7)	0.8(1)
O(19)	0.263(1)	0.25	0.461(1)	2.0(3)

[a] These atoms were refined anisotropically; they are given with the isotropic equivalent

$$B = 4/3 \sum_j \sum_i a_i \cdot a_j \cdot \beta_{ij}.$$

The other atoms are refined isotropically.

by replacing octahedra by PO_4 tetrahedra in an ordered way, as shown from the comparison of one (010) layer of polyhedra, $[Nb_2PO_8]_\infty$ (Fig. 2a), with one (001) layer of WO_6 octahedra, $[W_3O_9]_\infty$, of the HTBs (Fig. 2b). It can indeed be seen that the geometry and disposition of the chains of corner-sharing polyhedra running along **a** (labeled A) are the same in the two structures: the A chains of the $[Nb_2PO_8]_\infty$ layers are deduced from those of the $[W_3O_9]_\infty$ layers by replacing one octahedron out of four with one PO_4 tetrahedron. The rows of octahedra that connect two A chains in the HTBs (labeled B in Fig. 2b) are replaced by PO_4 tetrahedra in the following way: one row out of two (labeled B in Fig. 2a) remains untouched, the second row being replaced by a row of PO_4 tetrahedra (labeled B′ in Fig. 2a). As a result, one observes six-sided rings (labeled HTB in Fig. 2a) similar to those observed in HTB and built up from five NbO_6 octahedra and one PO_4 tetrahedron, and seven-sided rings (labeled S in Fig. 2a) built up from three PO_4 tetrahedra and four NbO_6 octahedra. Thus, one row of HTB rings out of two running along **a** in the HTB layers (Fig. 2b) is replaced by one row of seven-sided rings (Fig. 2a).

The $[Nb_2PO_8]_\infty$ framework is built up from the stacking along **b** of identical $[Nb_2PO_8]_\infty$ layers that share the corners of their polyhedra, as shown from the view of the structure along **a** (Fig. 3a). From the latter projection, it can be seen that one layer (labeled L) is connected in a different way to the identical adjacent layers above (labeled L′) and below (labeled L″) it. The L and L″ have their PO_4 tetrahedra pointing in opposite directions, so that they share only the corners of their octahedra, as in HTBs; consequently, in the couple "L–L″" the HTB rings are superposed along **b** (and of course the seven-sided rings are superposed). In contrast, the L and L′ layers have their PO_4 tetrahedra pointing toward each other, so that one PO_4 tetrahedron of one layer L is connected with one NbO_6 octahedron of the next layer L and vice versa; as a result, in the couple "L–L″" one HTB ring is superposed with a seven-sided ring. This sequence is reproduced all along **b** so that the large tunnels running along that direction result from the stacking of two HTB rings with two seven-sided rings alternately. The similarity with the HTBs is also seen by comparing the view of this structure along **a** (Fig. 3a) with that of the HTBs along the ⟨100⟩ direction (Fig. 3b).

The $[W_3O_9]_\infty$ framework consists of ReO_3-type chains $[WO_3]_\infty$ running along **c**. In the $[Nb_2PO_8]_\infty$ framework, one

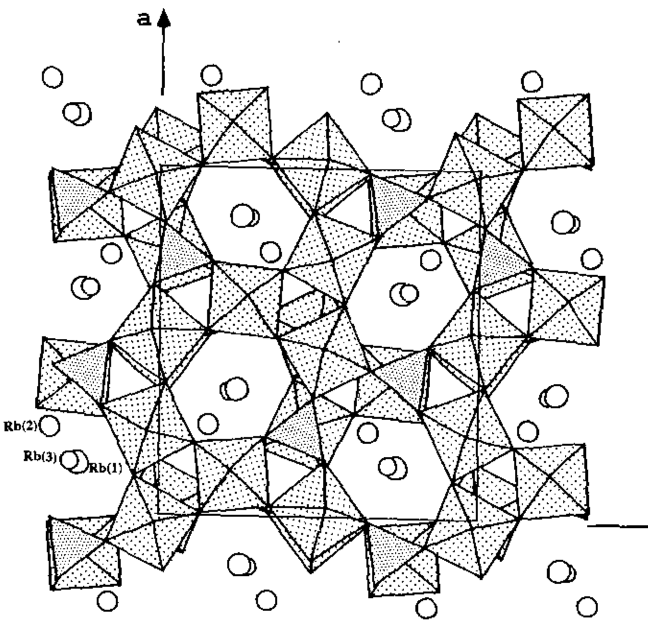

FIG. 1. Projection along **b** of $RbNb_2PO_8$.

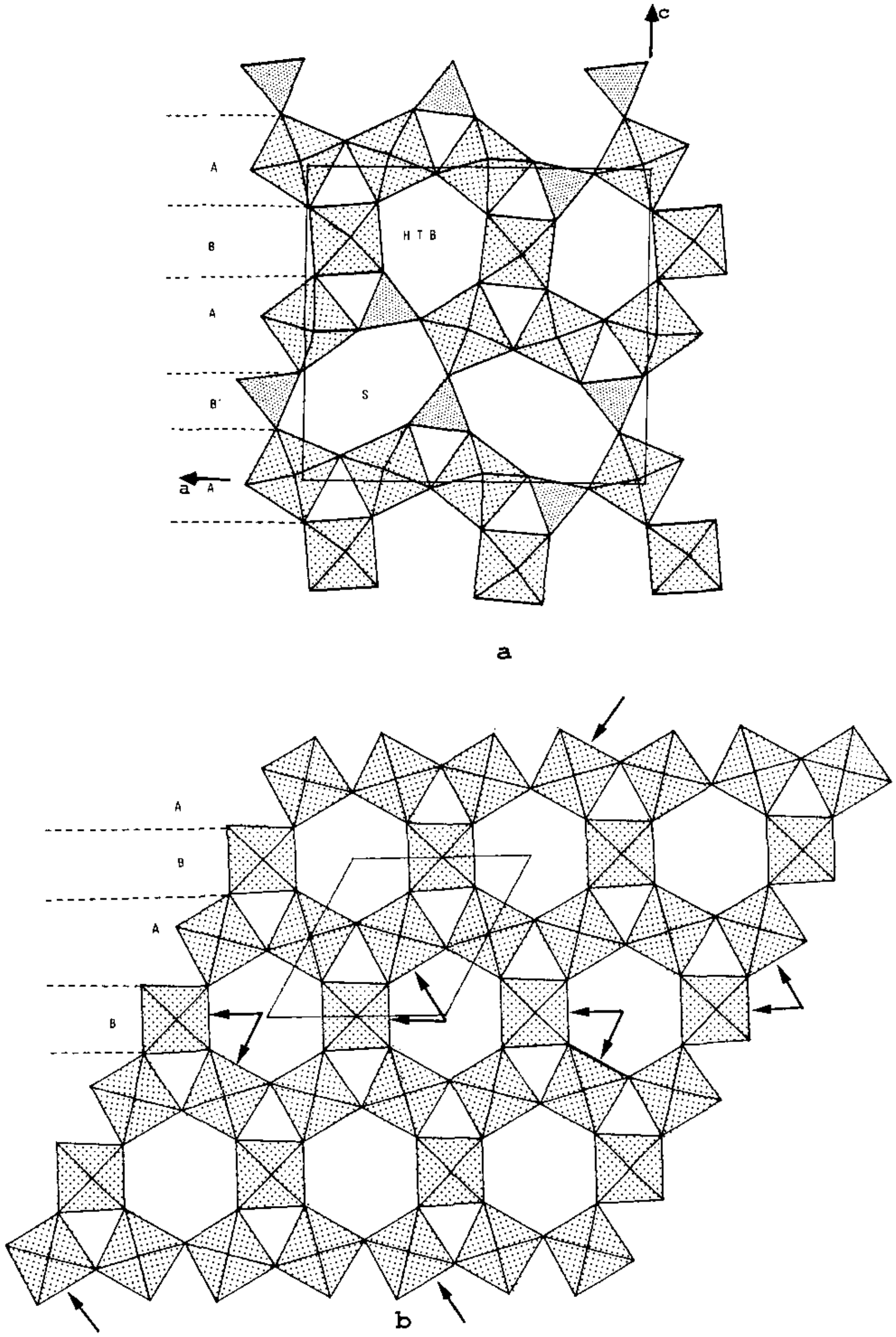

FIG. 2. (a) One (010) layer of the $[Nb_2PO_8]_\infty$ frameworks. (b) A HTB layer. The arrows show the octahedra replaced by tetrahedra in $RbNb_2PO_8$.

ReO_3-type chain, $[NbO_3]_\infty$, out of three is maintained, whereas the other adjacent octahedral chains running along **b** are replaced by mixed rows of PO_4 tetrahedra and NbO_6 octahedra forming $Nb_2P_2O_{17}$ strings, parallel to **b** of two NbO_6 octahedra and two PO_4 tetrahedra sharing their apices. In fact, one row of $Nb_2P_2O_{17}$ strings running along **b** (Fig. 4a) in the niobium phosphate is deduced from a ReO_3-type chains (Fig. 4b) just by replacing two octahedra out of four by PO_4 tetrahedra according to the sequence P–Nb–Nb–P . . . P–Nb–Nb–P. This substitution of P for W (or Nb) in the ReO_3-type chains leads to the creation of anionic vacancies, so that one observes

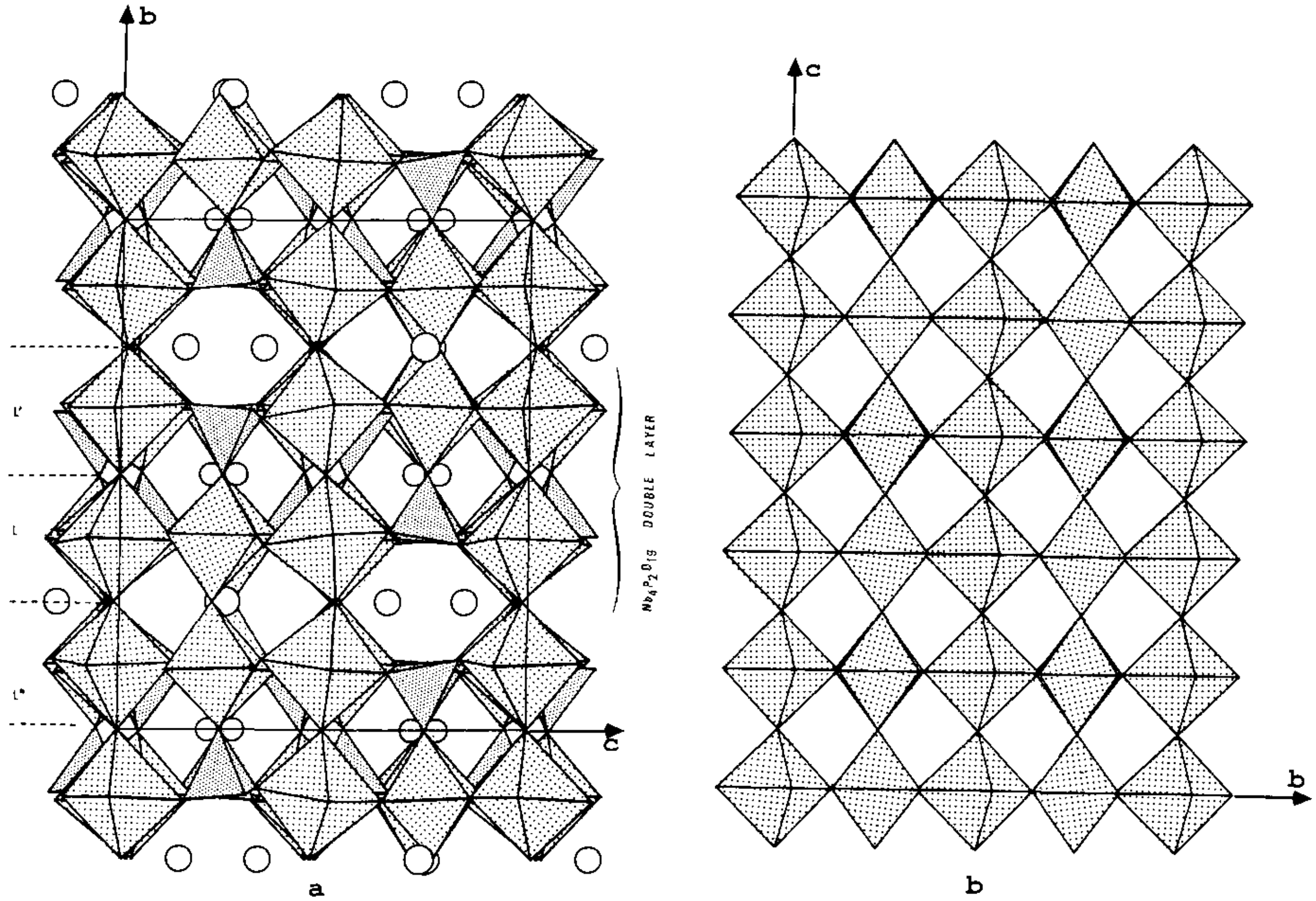

FIG. 3. (a) Projection along **a** of $RbNb_2PO_8$ showing the brownmillerite tunnels. (b) Projection along ⟨100⟩ of the HTB structure.

six-sided tunnels running along **a** in the phosphoniobate $RbNb_2PO_8$ (Fig. 3a). Note that these tunnels built up from two PO_4 tetrahedra and four NbO_6 octahedra are similar to those observed in the brownmillerite structure, and that they intersect the larger tunnels running along **b**.

It is worth pointing out that this framework exhibits the octahedral Nb_6O_{27} units (Fig. 5a) previously observed for $BaNb_7P_6O_{33}$ (10), $Ca_{0.5}Cs_2Nb_6P_3O_{24}$ (8), and $Na_6Nb_8P_5O_{35}$ (4), the structures of which are closely related to TTBs and HTBs. In $RbNb_2PO_8$, another kind of unit $Nb_4P_2O_{23}$ is also observed (Fig. 5b) that derives from the Nb_6O_{27} unit by replacing two NbO_6 octahedra with two PO_4 tetrahedra. Note also that the $Nb_2P_2O_{17}$ strings were previously observed in $CaNb_2P_2O_{11}$ (11).

The geometry of the two independent PO_4 tetrahedra is characteristic of the monophosphate groups with P–O distances ranging from 1.51 to 1.55 Å, and O–P–O distances ranging from 105.8 to 112.7° (Table 4).

Examination of the Nb–O distances (Table 4) allows two different geometries of the NbO_6 octahedra to be distinguished. The Nb(1) and Nb(2) octahedra that form the ReO_3-type chains exhibit one abnormally short apical Nb–O bond along **b** (1.74 to 1.79 Å), whereas the opposite Nb–O distance is very long (2.21 to 2.26 Å), the four other intermediate distances of the basal plane ranging from 1.86 to 2.14 Å.

Such a geometry, corresponding to almost regular O_6 octahedra in which the Nb atoms are off-centered along one direction of the ReO_3-type chains, has already been observed in several other niobium phosphates, such as $CsNbOP_2O_7$ (12), $K_3Nb_2PO_9$ (13), and $Tl_2NbO_2PO_3$ (14) and can be considered characteristic of niobyl ions. Note that two split sites are observed for the niobium ions in the chains, above and below the basal plane of the NbO_6 octahedra; consequently, in one chain the Nb atoms occupy one of these two sites (for instance, all above the basal plane) so that one short Nb–O bond alternates with a longer Nb–O bond along **b**, whereas in another chain they all sit in the opposite direction (i.e., all below the basal plane). Nevertheless, the displacements of the Nb atoms of these chains do not respect the crystal translation so that the two kind of sites (below and above the basal plane) are half occupied.

The Nb(3) and Nb(4) octahedra that form the $Nb_2P_2O_{17}$

TABLE 4
Distances (Å) and Angles (°) in the Polyhedra

Nb(1a)	O(1)	O(2)	O(3)	O(4)	O(5)	O(6)
O(1)	1.797(4)	2.67(1)	3.99(2)	3.20(1)	3.06(1)	2.67(1)
O(2)	92.1(4)	1.91(1)	2.81(2)	2.80(1)	3.95(2)	3.03(1)
O(3)	167.5(5)	85.4(6)	2.214(4)	2.71(2)	2.77(2)	2.70(2)
O(4)	113.1(4)	90.4(4)	79.3(6)	2.04(1)	2.57(1)	3.94(2)
O(5)	104.0(4)	162.6(5)	80.3(6)	77.3(4)	2.08(1)	2.78(1)
O(6)	89.2(4)	101.3(4)	79.3(6)	154.6(5)	85.8(4)	2.01(1)
Nb(1b)	**O(1)**	**O(2)**	**O(3)**	**O(4)**	**O(5)**	**O(6)**
O(1)	2.268(4)	2.67(1)	3.99(2)	3.20(1)	3.06(1)	2.67(1)
O(2)	79.0(4)	1.91(1)	2.81(2)	2.80(1)	3.95(2)	3.03(1)
O(3)	168.6(6)	100.4(7)	1.739(4)	2.71(2)	2.77(2)	2.70(2)
O(4)	97.7(4)	92.3(4)	93.7(7)	1.97(1)	2.57(1)	3.94(2)
O(5)	89.6(4)	164.6(5)	92.8(7)	78.8(4)	2.07(1)	2.78(1)
O(6)	77.2(4)	101.4(4)	91.9(7)	164.1(4)	86.0(4)	2.01(1)
Nb(2a)	**O(7)**	**O(8)**	**O(9)**	**O(10)**	**O(11)**	**O(12)**
O(7)	1.87(1)	2.76(1)	2.68(1)	2.80(1)	3.97(2)	2.82(2)
O(8)	89.9(5)	2.04(1)	3.97(2)	2.69(1)	2.95(1)	2.80(2)
O(9)	88.7(4)	164.7(6)	1.97(1)	2.93(1)	2.84(1)	2.87(2)
O(10)	84.8(4)	77.2(3)	87.5(4)	2.258(3)	2.89(1)	4.00(2)
O(11)	167.0(5)	90.2(4)	87.8(4)	82.6(3)	2.12(1)	2.78(2)
O(12)	101.9(7)	94.8(7)	100.3(7)	169.7(6)	91.0(6)	1.762(5)
Nb(2b)	**O(7)**	**O(8)**	**O(9)**	**O(10)**	**O(11)**	**O(12)**
O(7)	1.86(1)	2.76(1)	2.68(1)	2.80(1)	3.97(2)	2.82(2)
O(8)	90.0(5)	2.04(1)	3.97(2)	2.69(1)	2.95(1)	2.80(2)
O(9)	89.5(5)	168.3(6)	1.95(1)	2.93(1)	2.84(1)	2.87(2)
O(10)	99.9(4)	88.7(3)	102.9(4)	1.794(4)	2.89(1)	4.00(2)
O(11)	165.7(5)	89.7(4)	88.0(4)	94.4(3)	2.14(1)	2.78(2)
O(12)	86.7(6)	81.9(6)	86.4(6)	168.6(5)	79.2(5)	2.230(5)
Nb(3)	**$O(6^{i})$**	**$O(9^{ii})$**	**O(13)**	**O(14)**	**O(15)**	**O(16)**
$O(6^{i})$	1.85(1)	2.76(1)	2.80(2)	2.84(2)	3.95(2)	2.76(1)
$O(9^{ii})$	95.5(4)	1.88(1)	2.77(2)	2.73(2)	2.77(1)	3.89(2)
O(13)	95.9(6)	94.1(6)	1.914(3)	3.96(2)	2.81(1)	2.75(1)
O(14)	93.1(6)	87.8(5)	170.5(6)	2.06(1)	2.75(2)	2.85(2)
O(15)	174.3(5)	88.0(4)	88.3(5)	82.5(5)	2.11(1)	2.80(1)
O(16)	90.9(4)	172.9(4)	88.6(6)	88.6(5)	85.4(4)	2.02(1)
Nb(4)	**$O(2^{iii})$**	**O(7)**	**$O(16^{iv})$**	**O(17)**	**O(18)**	**O(19)**
$O(2^{iii})$	1.94(1)	3.90(2)	2.79(1)	2.75(2)	3.04(1)	2.72(2)
O(7)	177.7(4)	1.96(1)	2.65(1)	2.87(2)	2.75(1)	2.72(2)
$O(16^{iv})$	94.6(4)	87.8(4)	1.86(1)	2.81(2)	4.02(2)	2.90(2)
O(17)	87.6(5)	92.2(6)	92.5(5)	2.03(1)	2.67(2)	3.90(2)
O(18)	94.7(4)	82.9(4)	166.9(4)	78.7(5)	2.19(1)	2.85(2)
O(19)	90.3(8)	89.4(8)	101.0(7)	166.5(7)	88.2(7)	1.898(2)

P(1)	O(4)	O(8)	O(14)	O(18)
O(4)	1.55(1)	2.48(1)	2.49(2)	2.51(1)
O(8)	105.8(6)	1.55(1)	2.53(2)	2.55(1)
O(14)	107.8(7)	110.4(7)	1.53(1)	2.55(2)
O(18)	108.7(6)	111.2(6)	112.7(8)	1.53(1)

TABLE 4—*Continued*

P(2)	$O(5^{iv})$	$O(11^{ii})$	O(15)	O(17)
$O(5^{iv})$	1.51(1)	2.50(1)	2.44(1)	2.48(2)
$O(11^{ii})$	109.9(6)	1.54(1)	2.54(1)	2.49(2)
O(15)	106.8(6)	111.7(6)	1.53(1)	2.50(2)
O(17)	109.8(8)	108.7(7)	110.0(6)	1.52(1)

Note. The Nb–O or P–O distances are on the diagonal. Above it are the O(*i*) . . . O(*j*) distances and below it are the O(*i*)–Nb–O(*j*) or O(*i*)–P–O(*j*) angles.

$Rb(1)–O(6^{v})$	= 3.20(1)	Rb(2)–O(4)	= 3.05(1)	$Rb(3)–O(2^{iii})$	= 3.27(1)
$O(6^{iv})$	= 3.20(1)	$O(4^{ix})$	= 3.05(1)	$O(7^{vii})$	= 3.36(1)
$O(7^{vi})$	= 3.36(1)	O(5)	= 3.18(1)	$O(8^{iii})$	= 2.92(1)
$O(7^{vii})$	= 3.36(1)	$O(5^{ix})$	= 3.18(1)	$O(9^{vii})$	= 3.35(1)
$O(9^{vi})$	= 3.14(1)	$O(11^{x})$	= 2.95(1)	$O(10^{iii})$	= 3.43(1)
$O(9^{vii})$	= 3.14(1)	$O(11^{iii})$	= 2.95(1)	$O(11^{iii})$	= 3.15(1)
O(13)	= 3.18(1)	$O(12^{iii})$	= 3.39(1)	O(14)	= 3.47(2)
O(15)	= 2.98(1)	O(18)	= 2.96(1)	$O(14^{iii})$	= 3.48(2)
$O(15^{viii})$	= 2.98(1)	$O(18^{ix})$	= 2.96(1)	O(15)	= 2.99(1)
O(16)	= 3.42(1)			O(16)	= 3.08(1)
$O(16^{viii})$	= 3.42(1)			O(17)	= 3.24(1)
				O(18)	= 3.24(1)

Symmetry codes

i	:	$-x$	$1-y$	$-z$
ii	:	$-x$	$1-y$	$1-z$
iii	:	$\frac{1}{2}+x$	y	$\frac{1}{2}-z$
iv	:	$\frac{1}{2}-x$	$1-y$	$\frac{1}{2}+z$
v	:	$\frac{1}{2}-x$	$\frac{1}{2}+y$	$\frac{1}{2}+z$
vi	:	$\frac{1}{2}-x$	$\frac{1}{2}+y$	$z-\frac{1}{2}$
vii	:	$\frac{1}{2}-x$	$1-y$	$z-\frac{1}{2}$
viii	:	x	$\frac{3}{2}-y$	z
ix	:	x	$\frac{1}{2}-y$	z
x	:	$\frac{1}{2}+x$	$\frac{1}{2}-y$	$\frac{1}{2}-z$

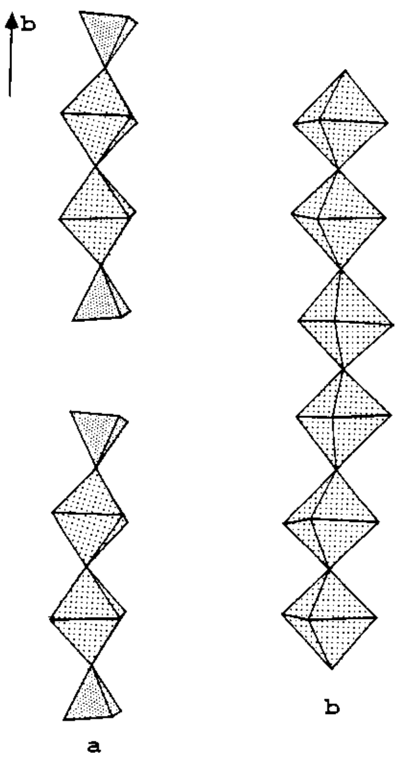

FIG. 4. (a) The $Nb_2P_2O_{17}$ string running along **b**. (b) The ReO_3 chain running along **b**.

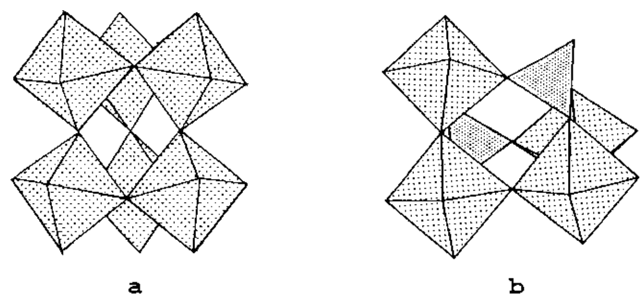

FIG. 5. (a) Nb_6O_{27} unit; (b) $Nb_4P_2O_{23}$ unit.

strings exhibit a much less pronounced difference between their Nb–O distances (Table 4), which range from 1.85 to 2.11 Å and from 1.86 to 2.19 Å, respectively.

The rubidium ions are located in the tunnels. Rb(1) and Rb(3) sit near the axis of the tunnels running along **b** (Fig. 1). They are surrounded by 11 and 12 oxygen atoms, respectively, with Rb–O distances ranging from 2.99 to 3.48 Å (Table 4). The Rb(2) ions are located at the intersection of the two sorts of tunnels running along **b** and **a**, respectively. These cations exhibit a ninefold coordination with Rb–O distances ranging from 2.95 to 3.18 Å.

The calculated valence sums, based on the Nb–O and Rb–O distances using the Brown and Altermatt formula (15), confirm the valence (V) for niobium (4.92 to 5.2).

CONCLUDING REMARKS

The perfectly ordered substitution of PO_4 tetrahedra for NbO_6 octahedra in the hexagonal tungsten bronze structure has been demonstrated for the first time. This suggests that many other mixed frameworks derived from the HTBs by introducing PO_4 tetrahedra should be synthesized in the future. A systematic investigation of such derivatives is in progress. The existence of intersecting tunnels suggests ionic mobility, which will be investigated.

REFERENCES

1. J. P. Giroult, M. Goreaud, Ph. Labbé, and B. Raveau, *Acta Crystallogr., Sect. B* **37,** 2139 (1981).
2. J. P. Giroult, M. Goreaud, Ph. Labbé, and R. Raveau, *J. Solid State Chem.* **50,** 163 (1983).
3. A. Leclaire, M. M. Borel, A. Grandin, and B. Raveau, *J. Solid State Chem.* **80,** 12 (1989).
4. A. Benabbas, M. M. Borel, A. Grandin, A. Leclaire, and B. Raveau, *J. Solid State Chem.* **92,** 51 (1991).
5. A. Leclaire, A. Benabbas, M. M. Borel, A. Grandin, and B. Raveau, *J. Solid State Chem.* **83,** 245 (1989).
6. A. Benabbas, M. M. Borel, A. Grandin, A. Leclaire, and B. Raveau, *J. Solid State Chem.* **84,** 365 (1990).
7. A. Benabbas, M. M. Borel, A. Grandin, A. Leclaire, and B. Raveau, *J. Solid State Chem.* **87,** 360 (1990).
8. G. Costentin, M. M. Borel, A. Grandin, A. Leclaire, and B. Raveau, *J. Solid State Chem.* **90,** 279 (1991).
9. A. Magneli, *Acta Chem. Scand.* **7,** 315 (1953).
10. G. Costentin, M. M. Borel, A. Grandin, A. Leclaire, and B. Raveau, *J. Solid State Chem.* **93,** 46 (1991).
11. D. L. Serra and S. Hwu, *J. Solid State Chem.* **98,** 174 (1992).
12. V. P. Nokolaev, G. G. Sadivok, A. V. Lavrov, and M. A. Porai-Koshits, *Dokl. Akad. Nauk SSSR* **264,** 859 (1982).
13. M. F. Zid and I. Jouini, *J. Solid State Chem.* **99,** 201 (1992).
14. M. Fakhfakh, M. F. Zid, N. Jouini, and M. Tournoux, *J. Solid State Chem.* **102,** 368 (1993).
15. I. D. Brown and D. Altermatt, *Acta Crystallogr., Sect. B* **41,** 244 (1985).